

Detector Upgrade of Subaru’s Multi-Object Infrared Camera and Spectrograph (MOIRCS)

Maximilian Fabricius^a, Josh Walawender^{a,b}, Nobuo Arimoto^a, David Cook^a, Brian Elms^a, Yasuhito Hashiba^c, Takashi Hattori^a, Yen-Sang Hu^d, Ikuru Iwata^a, Tetsu Nishimura^a, Koji Omata^a, Philip Tait^a, Naruhisa Takato^a, Ichi Tanaka^a, Shiang-Yu Wang^d, Mark Weber^a, and Matthew Wung^a

^aSubaru Telescope (NAOJ), 650 North Aohoku Place, Hilo, HI 96720, USA

^bW. M. Keck Observatory, 65-1120 Mamalahoa Hwy, Waimea, HI 96743, USA

^cInstitute of Astronomy, University of Tokyo, 2-21-1 Osawa, Mitaka, Tokyo 181-0015, Japan

^dAcademica Sinica, Institute for Astronomy and Astrophysics, 11F of AS/NTU Astronomy-Mathematics Building, No.1, Sec. 4, Roosevelt Rd, Taipei 10617, Taiwan, R.O.C.

ABSTRACT

During the past year, the Multi-Object InfraRed Camera and Spectrograph at Subaru has undergone an upgrade of its science detectors, the housekeeping electronics and the instrument control software. This overhaul aims at increasing MOIRCS’ sensitivity, observing efficiency and stability. Here we present the installation and the alignment procedure of the two Hawaii 2RG detectors and the design of a cryogenic focus mechanism. The new detectors show significantly lower readnoise, increased quantum efficiency, and lower the readout time.

Keywords: MOIRCS, Subaru, near-infrared, imaging, spectroscopy, MOS, H2RG, Hawaii 2RG

1. INTRODUCTION

The Multi-Object InfraRed Camera and Spectrograph^{1,2} is Subaru’s workhorse instrument for seeing limited observations in the near-infrared. By dividing its field of view through a roof mirror system into two identical channels, the instrument offers imaging in Y,J,H,K[s] with a field of view (FOV) of $7' \times 4'$ and Multi Object Spectroscopy (MOS) through cryogenic slit masks ($R = 500 - 3200$ for a $0.5''$ slit). For a description of the instrument please see the parallel presentation [3]. MOIRCS has been one of the earliest instruments of its kind (first light 2004, open use since 2005), but more recent instruments such as MOSFIRE⁴ offer a higher sensitivity. As part of the nuMOIRCS project, in 2015 MOIRCS has undergone an upgrade of its science detectors, housekeeping electronics, and instrument control system. Here we describe the replacement of the two older HgCdTe Hawaii II detectors by Teledyne’s more recent Hawaii 2RG (H2RG) models.

2. NEW DETECTORS AND READOUT SYSTEM

We purchased the new H2RG arrays from Teledyne Scientific Imaging. These detectors have 2048×2048 pixels with an edge size of $18 \mu\text{m}$ which is identical to the size of the older Hawaii II arrays such that no modification of the image scale was necessary. The outer four rows of pixels around each of the four edges of the detector are not sensitive to light but serve as reference pixels that allow to correct for the channel to channel reset level variation. The H2RG detectors have 32 readout channels which in principle results in a factor of 8 increase in readout speed over the older 4 channel system ($\simeq 100\text{kHz}$ readout). Further improvements of the new detector generation are a lower readnoise and an improved quantum efficiency towards lower wavelengths due to the removal of the detector substrate on the H2RG model.

We obtained a total of three science grade detectors with the third one serving as spare. We employ the SIDECAR ASIC^{5,6} for the detector readout in combination with the current SAM readout electronics, both from Teledyne Scientific.

Further author information: (Send correspondence to M.F.)
M.F.: E-mail: mxhf@naoj.org

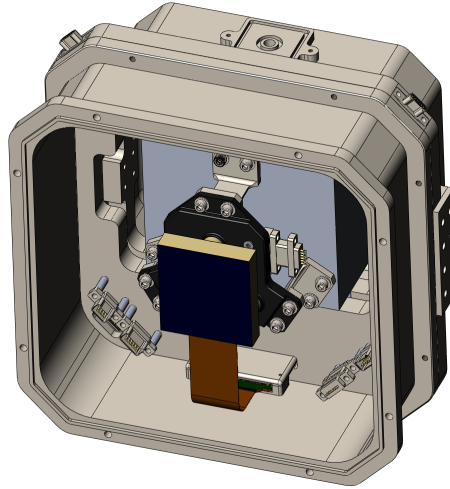


Figure 1. A rendered image of the GLS detector module. The module provides the mounting interface for the detector, a light tight enclosure, heaters, temperature sensors and electrical connections.

3. DETECTOR HOUSING

We purchased the detector modules from GL Scientific, Inc. (GLS). The modules provide a light tight enclosure around the detector and a mount for the detector and the Sidecar ASIC. They include resistive heaters and temperature sensors, one for the detector and a higher power one for the module. Finally, they include appropriate feedthroughs for the detector signals, the temperature control and the focus drive limit switches.

4. INTERFACE TO THE OPTICAL BENCH

A single piece aluminium window frame (see Fig. 2) mounts the detector modules onto the optical bench. We incorporated reference surfaces for the tip/tilt, piston and lateral alignment of the detectors. Two G10 brackets between the window frame and the module insulate the module from the optical bench. The image plane of MOIRCS is tilted by 0.39 degree. The surface of the frame that faces the optical bench is tilted correspondingly.

5. FOCUS DRIVE

MOIRCS has been equipped with a focus z-drive. The internal focus of MOIRCS, i.e. the relative focus between the MOS image plane and the detector image plane proved to be very stable over time. However, some minor drifts in the order of $50\ \mu\text{m}$ are observed after a warm up of the instrument such that a focus drive is needed to readjust. In addition to counteracting the degradation of image quality through defocus, the existence of a focus drive also greatly simplifies the procedure of the detector tip/tilt alignment (see the following section).

The previous focus drive was incompatible with the new detector modules such that we had to design a new mechanism that was mechanically compatible with the modules (see Fig. 3). Specifically, they had to fit into the limited space that was available behind the detectors. In our design a triangular base stage slides back and forth on three rods. A nutblock is placed inside the base stage and a stepper motor directly drives a lead screw to push the stage back and forth. An additional triangular plate that is connected to the main stage via three standoffs provides the mounting base for the detector. Braided copper straps provide a thermal connection between the detector housing and the mounting base. All metal parts are machined out of 6061 aluminum. The nutblock and the bushings around the rods are machined out of Vespel. We used Phytron (model VSS 52.200.2.5-UHVC-4Lp), cryogenic stepper motors and the Phytron phyMOTION motor controller. Forward and backward limit switches provide an absolute position reference and additional hardstops protect the detector from damage by accidental out-of-range motion.

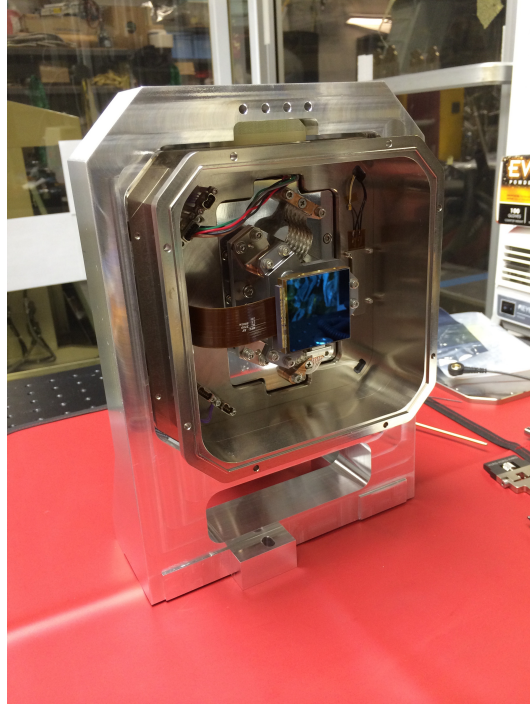


Figure 2. This photograph shows the array module integrated into the window frame that mounts onto the optical bench of MOIRCS. The yellow piece of material on the top is a G10 bracket that provides thermal insulation between the module and the frame. There is a corresponding second bracket at the bottom of the module that is hidden in this view.

We tested the focus stages under room temperature for tip/tilt stability and position repeatability. The tip/tilt error upon return to the same position is less than five arcminutes and the position repeatability lies five microns which is sufficiently small to cause no measurable degradation in image quality across the detector. We also tested the stages extensively under cryogenic conditions before the installation in the instrument. For short cycle test we cooled the stage with liquid nitrogen and for full function test we employed a test dewar with a cryogenic closed cycle cooler. This led to several modifications in the original design. We found that we had to remove a collar from the bushings that led to “gripping” of the bushings onto the rods at 77 K. Also, we found that it was necessary to open up the thread of the nutblock to avoid strong gripping of the nutblock onto the leadscrew. In fact, this was simply achieved by re-tapping the block repeatedly immediately after dipping it in liquid nitrogen.

6. DETECTOR ALIGNMENT

Each precool of MOIRCS requires about 1600 l of liquid nitrogen and takes 72 hours. While Subaru has developed an automated precool system to eliminate manual tank changes during night time,⁷ the precool still requires day and night monitoring by observatory personnel. Therefore it was desirable to implement a strategy to align the detectors with very few iterations, as each iteration required another precool.

The existence of the focus drive allows us to collect a focus series where the detector is moved through its full range of motion. We utilize a special MOS mask that has 96 pinholes, evenly distributed across each detector field of view. By measuring the spot size at a series of focus positions we obtain 96 separate focus curves. Their minima give the absolute location of the actual image focal plane of MOIRCS. We implemented a numerical procedure in python that derives the focal plane location mostly automatically from a set of images of a focus series. Relatively minor manual interaction is required to reject curves of a few individual pinholes that are affected by nearby hot pixels. The routine models each focus curve as a parabola where the minimum, the location of the minimum, and the steepness of the parabola are free parameters. The location of the minima

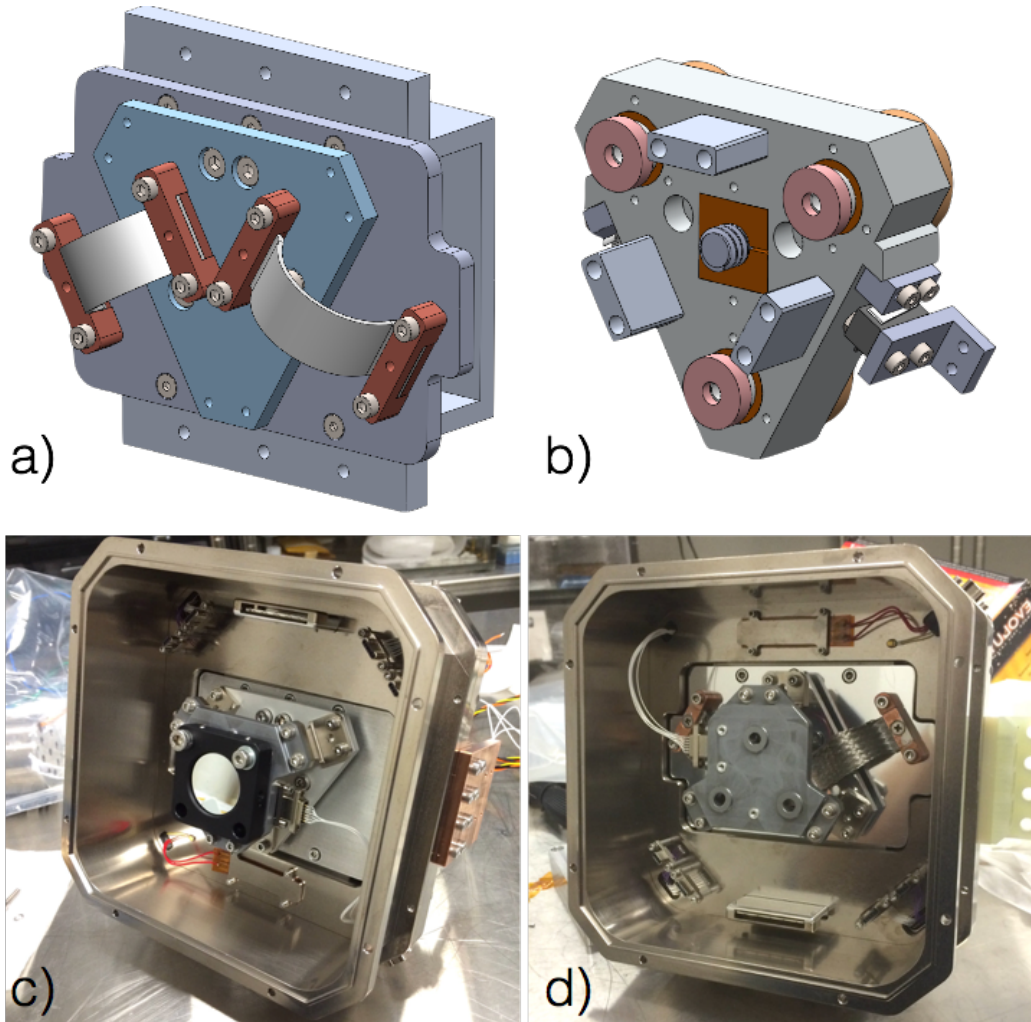


Figure 3. The new focus stage. *a)* shows a rendered image of the focus drive with the triangular mounting plate for the detector and two braided copper straps. *b)* presents the internal structure of the focus stage. The base plate moves along three cylindrical rods. Vespel bushings provide a low friction interface between the rods and the stage. The endcaps that are seen here on the rods (drawn in red) are precise hardstops to protect the detector from mechanical damage. Two limit switches serve as absolute position reference. The stage is driven by a lead screw that is coupled directly to the shaft of the cryogenic stepper. *c)* shows the focus drive installed into the GLS detector module. We mounted a mirror instead of the detector to test tip/tilt stability and repeatability. *d)* shows again the module with the focus drive. But now the cooling straps are installed and the module is ready for the integration of the detectors.

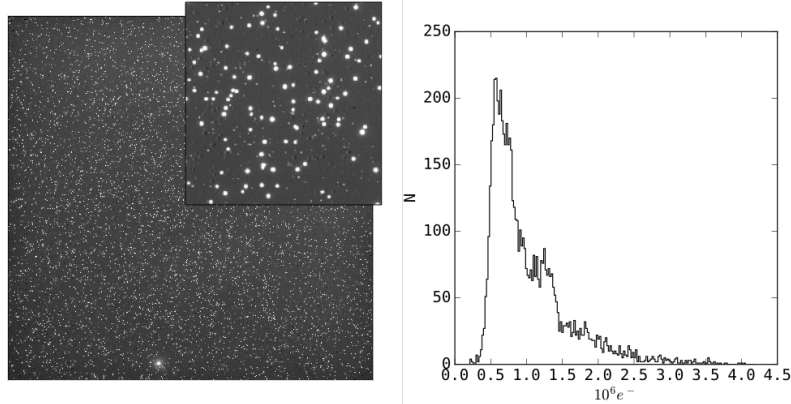


Figure 4. The left image shows a 10 min. dark exposure after the first installation of the new detectors in MOIRCS. Radiation events are seen distributed mostly homogeneously across the detector. The inset shows a zoom-in on the central region of the detector. The plot on the right shows a histogram of the signal of the radiation events. The main peak lies at about 590 ke^- . The secondary peak at about 1200 ke^- is a result of double counts. Note that the events do saturate the detector and that the detector becomes significantly non-linear at such high signal levels. Therefore a derivation of the actual radiation energy is difficult.

across all pinholes is then modelled by a simple three dimensional plane which corresponds to the image focal plane. The z position of the plane and its tip and tilt are fitted together with the other parameters through a standard least squares algorithm (`scipy.optimize.leastsq`). With the location of the focal plane at hand we returned to the 3D design of the detector mount and introduced a virtual plane to mark the focal plane location. We then adjusted the detector location to be aligned with that virtual plane. As the position of the detector module and the window frame are tied to the detector position, this allowed us to “measure” in the 3D design the required shim thickness between the reference surfaces on the window frame, the optical bench and the upstream field lens mount. We then proceeded to warm and open MOIRCS to install those shims of computed thicknesses and continued with another precool to verify the improved detector location.

Unfortunately an incorrect wiring of one of the focus stepper motors initially led to a shimming in the wrong direction in one of the channels. But after three iterations (three precools) we achieved a detector tip/tilt offset of under $5'$ which is at the limit of what we can measure reliably from a focus series. More importantly this residual tilt results in a well acceptable image quality across the detector. The FWHM of the internal PSF across the detector is 1.2 pixel on average which corresponds to $0.14''$.

7. H2RG DETECTORS ARE α -PARTICLE DETECTORS

After the installation of the detectors into MOIRCS we were surprised to see what looked like a large number of cosmic ray hits. They were, however, fairly energetic events with about 590 ke of signal per event and appeared at a very high rate of several dozens over a 10 s integration. Based on reports of a similar experience at the neighboring NASA Infrared Telescope Facility (IRTF) during the upgrade of their SPeX instrument (Michael Connelley, priv. communication, see also [8]) we immediately suspected alpha particle radiation emanating from the ThF4 anti-reflective coating of the last lens surface in front of the detector.

One of the significant advances of the H2RG generation of Teledyne’s Hawaii detectors is the removal of the backside substrate after the growth of the photosensitive HgCdTe material through molecular beam epitaxy. This led to a significant increase in the detectors quantum efficiency towards shorter wavelengths. However the removal of the substrate also led these new detectors to become very sensitive α particle detectors.

Initially we explored options to remove the ThF4 coating from the last lens and to replace it with a non-radioactive coating. Unfortunately, the sensitivity of the material of the last lens (BaF2) and its very steep curvature made this prohibitively expensive. As however the interaction probability of α particles with just about any material is very high its penetration depth is very low. It was therefore clear that a thin glass window

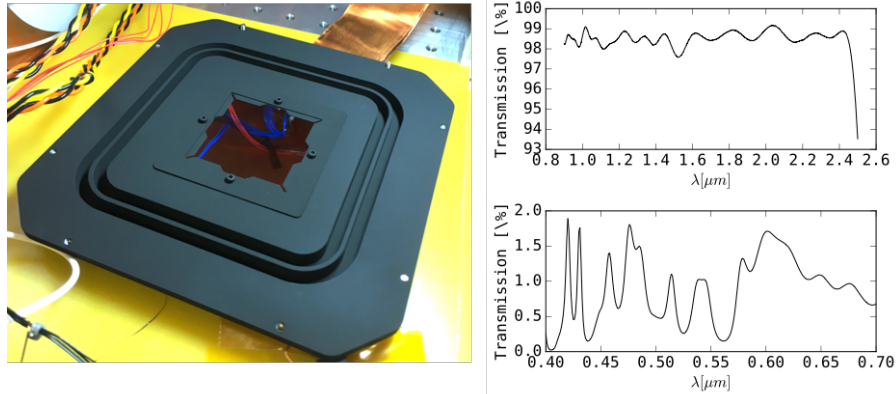


Figure 5. The left image shows the α blocking filter, integrated in a light baffle that is mounted directly in front of the detector. In this image the filter and baffle are installed in one of Subaru’s test dewars for cryogenic testing. The plots on the right show the transmission of the filter in the blocking and the non-blocking wavelength regions.

would block the radiation very effectively. Only, in order to avoid a too large difference in optical path length, the filter had to be relatively thin and, in order to prevent ghosting, a high quality anti-reflective coating had to be applied. We purchased Infrasil filters from Asahi Spectra Japan. Asahi was able to apply a broad band anti-reflective (BBAR) coating on both sides of the filter which results in an average transmission of 98.5% with very little ripple (97.6% minimum 99.2% maximum) across the entire wavelength range of 0.9 μm to 2.4 μm . The filters are 50 mm \times 50 mm in size with a thickness of only 1 mm. The manufacturer achieved a transmitted peak-to-valley wavefront error of 0.07 waves.

Incidentally BaF₂ is used a scintillator material in α particle detectors. The BaF₂ optics of MOIRCS should constantly emit a low level of blue light, to which the new substrate removed H₂RGs are actually sensitive to some degree. We estimated that the signal level of the scintillation glow is just about at the limit of what we can detect, but given that we applied a broad band coating to the blocking filter in any case, we could just as well also make it blocking at visible wavelengths. The transmission of the Asahi coating is on average 0.9% below 0.7 μm .

We opened MOIRCS one more time in March to install the filters which in subsequent tests indeed turned out to be effective at blocking the α radiation.

8. DETECTOR OPERATING PARAMETERS AND CHARACTERIZATION

We found that the differential readout mode with the non-enhanced clocking scheme and the row-per-row reset resulted in the lowest readnoise values for our system. A critical discovery was that the removal of the grounding pin to the readout computer was essential, not only to lower the readnoise by about 10e^- but also to avoid otherwise relatively frequent readout glitches (see also [6]). As [9] we do not make use of the kTC noise removal option as this actually worsened the noise performance.

We mostly use Teledyne’s standard operating voltages. We did however find that a lowered bias gate voltage (VBiasGate) results in a lower cross talk between channels (see [10]). We found that a value of 1.80 V led to negligible crosstalk for signal levels around half full well.

Following the manual, we tuned the reference voltage (VRefMain) to adjust the bias level to about 12000 counts. There is also some optimization with respect to the readnoise that can be achieved by tuning VRefMain (see Fig. 6), also we found that a value of more that 6500 counts is desirable to lower vertical striping.

We use the gain 10 setting, which according to the manual should result in a gain of about $2\text{e}^-/\text{ADU}$. From a photon transfer curve we did indeed derive values of $2.07\text{e}^-/\text{ADU}$ and $1.99\text{e}^-/\text{ADU}$ for channel 1 and channel 2 respectively. This is the value after the application of the 6% correction for inter pixel capacitance.

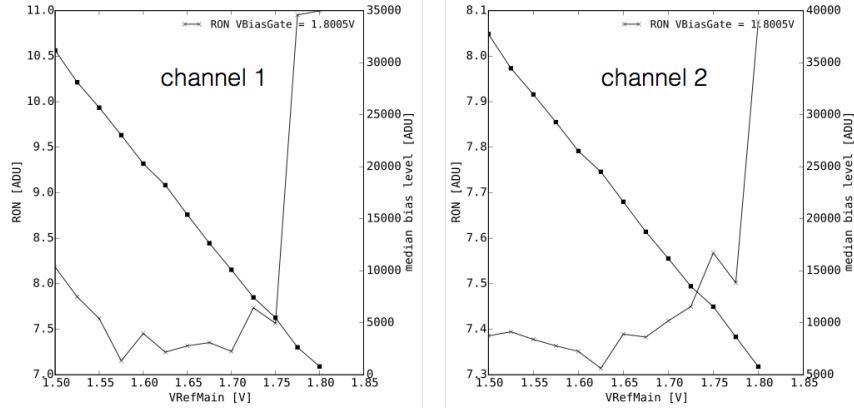


Figure 6. These plots show the results the change of bias level and readnoise for the two detectors. Too high values of VRefMain result in increased readnoise. We also find that this lead to a worsening of a vertical striping pattern. On the other hand, high bias values led to a lowered dynamic range.

With these operating parameters we obtain a single CDS noise of $13.9 e^-$ in channel 1 and $15 e^-$ using a pixel wise noise computation and a non-linearity of 1.7 % in channel 1 and 1 % in channel 2 at a signal level of $60 ke^-$ (about half full well).

9. NEW SYSTEM THROUGHPUT AND OBSERVING EFFICIENCY

A total of 7 engineering runs were assigned to MOIRCS from December 16, 2015 to June 17, 2016. The first nights still suffered from the α radiation problem and MOIRCS did not yet have the blocking filters installed. There we tested primarily the software functionality of first the imaging mode and then in the second run the MOS capability.

In May we were then able to conduct standard star observations with the alpha blocking filters in place. Table 1 lists the system throughput that we reach in the two channels. In imaging mode the throughput averages between 33 % and 40 % from Y to K band including telescope and atmospheric extinction. This represents a marginal increase at K band with respect to the old detectors only and a 5 % – 7 % increase at Y band which is of course owed primarily to the removal of the backside substrate from the new H2RG detectors. The parallel presentation [3] gives an update of the throughput in spectroscopy.

More importantly, the observing efficiency — the actual fractional time that MOIRCS is integrating signal — has been improved by 17 % to 30 % depending on the exact mode of observation. This is driven by the now 32 channel vs. the older 4 channel readout. Further improvements are expected by the future change to a new readout software that is expected to further lower the overhead from the setting of configuration parameters and from an optimization of the observing modes.

Table 1. Caption for the table.

Band	channel 1	channel 2
	[%]	[%]
Y	35.7	29.9
J	34.3	32.6
H	40.5	42.0
K	38.4	41.4

10. CONCLUSIONS

The detector upgrade of MORICS was concluded with the recent first open use observation on June 18, 2016, which was successfully completed with only minor software glitches. With the removal of MOIRCS from the

summit in April 2014 the total instrument downtime was 14 months. Out of these, 4 months were the result of the mitigation of the unexpected alpha radiation problem.

Overall, the improvement of sensitivity lags somewhat behind similar upgrades that were undertaken elsewhere, which shows that the prior detectors had a fairly high quantum efficiency to begin with. The improvement in readnoise is significant ($\simeq 30 \text{ e}^{-1}$ down to $\simeq 15 \text{ e}^{-1}$). This together with the increase in observing efficiency will increase the appeal of MOIRCS to the science community in the coming years.

ACKNOWLEDGMENTS

This work was made possible by funding support through a KAKENHI (23224005) Grant-in-Aid for Scientific Research (S) through the Japan Society for the Promotion of Science (JSPS) (PI: Nobuo Arimoto).

REFERENCES

- [1] Ichikawa, T., Suzuki, R., Tokoku, C., Uchimoto, Y. K., Konishi, M., Yoshikawa, T., Yamada, T., Tanaka, I., Omata, K., and Nishimura, T., “MOIRCS: multi-object infrared camera and spectrograph for SUBARU,” in [*Society of Photo-Optical Instrumentation Engineers (SPIE) Conference Series*], *SPIE* **6269**, 626916 (June 2006).
- [2] Suzuki, R., Tokoku, C., Ichikawa, T., Uchimoto, Y. K., Konishi, M., Yoshikawa, T., Tanaka, I., Yamada, T., Omata, K., and Nishimura, T., “Multi-Object Infrared Camera and Spectrograph (MOIRCS) for the Subaru Telescope I. Imaging,” *PASJ* **60**, 1347–1362 (Dec. 2008).
- [3] Walawender, J., Wung, M., Fabricius, M. H., Tanaka, I., Arimoto, N., Cook, D., Elms, B., Hashiba, Y., Hu, Y.-S., Iwata, I., Nishimura, T., Omata, K., Takato, N., Wang, S.-Y., and Weber, M., “The NuMOIRCS Project: Detector Upgrade Overview and Early Commissioning Results,” in [*Ground-based and Airborne Instrumentation for Astronomy VI*], *SPIE* **9908** (June 2016).
- [4] McLean, I. S., Steidel, C. C., Epps, H. W., Konidaris, N., Matthews, K. Y., Adkins, S., Aliado, T., Brims, G., Canfield, J. M., Cromer, J. L., Fucik, J., Kulas, K., Mace, G., Magnone, K., Rodriguez, H., Rudie, G., Trainor, R., Wang, E., Weber, B., and Weiss, J., “MOSFIRE, the multi-object spectrometer for infra-red exploration at the Keck Observatory,” in [*Ground-based and Airborne Instrumentation for Astronomy IV*], *SPIE* **8446**, 84460J (Sept. 2012).
- [5] Loose, M., Lewyn, L., Durmus, H., Garnett, J. D., Hall, D. N. B., Joshi, A. B., Kozłowski, L. J., and Ovsiannikov, I., “SIDE CAR low-power control ASIC for focal plane arrays including A/D conversion and bias generation,” in [*Instrument Design and Performance for Optical/Infrared Ground-based Telescopes*], Iye, M. and Moorwood, A. F. M., eds., *SPIE* **4841**, 782–794 (Mar. 2003).
- [6] Dorn, R. J., Eschbaumer, S., Hall, D. N. B., Finger, G., Mehrgan, L., Meyer, M., and Stegmeier, J., “Evaluation of the Teledyne SIDE CAR ASIC at cryogenic temperature using a visible hybrid H2RG focal plane array in 32 channel readout mode,” in [*High Energy, Optical, and Infrared Detectors for Astronomy III*], *SPIE* **7021**, 70210Q (July 2008).
- [7] Omata, K., Nishimura, T., Colley, S., Cook, D., Gorman, W., Magrath, B., Ramos, L., Kleinman, S., Tokoku, C., Konishi, M., Yoshikawa, T., Tanaka, I., and Suzuki, R., “Automatic pre-cooling system for large infrared instruments,” in [*Advanced Optical and Mechanical Technologies in Telescopes and Instrumentation*], *SPIE* **7018**, 70182E (July 2008).
- [8] Rayner, J., [*SpeX Observing Manual*] (2015).
- [9] Fox, O. D., Kuttyrev, A. S., Rapchun, D. A., Klein, C. R., Butler, N. R., Bloom, J., de Diego, J. A., Farah, A., Gehrels, N. A., Georgiev, L., González, J. J., Lee, W. H., Loose, M., Lotkin, G., Moseley, S. H., Prochaska, J. X., Ramirez-Ruiz, E., Richer, M. G., Robinson, F. D., Román-Zúñiga, C., Samuel, M. V., Sparr, L. M., and Watson, A. M., “Performance and calibration of H2RG detectors and SIDE CAR ASICs for the RATIR camera,” in [*High Energy, Optical, and Infrared Detectors for Astronomy V*], *SPIE* **8453**, 84531O (July 2012).
- [10] Simms, L. M., *Hybrid CMOS SiPIN detectors as astronomical imagers*, PhD thesis, University of Helsinki, Finland (2010).